Article:

Baco, S., Abbas, Q.A., Hayward, T.J. et al. (2021) An investigation on the mechanical properties of soft magnetostrictive FeCoCr films by nanoindentation. Journal of Alloys and Compounds, 881. 160549. ISSN: 0925-8388

https://doi.org/10.1016/j.jallcom.2021.160549

An investigation on the Mechanical Properties of Soft Magnetostrictive FeCoCr films by Nanoindentation

S. Baco[1,2], Q.A. Abbas[3], T.J. Hayward[1], N. A. Morley[1]

[1]Department of Materials Science and Engineering, University of Sheffield, Sheffield S1 3JD, UNITED KINGDOM.

[2]Programme of Industrial Physics, Faculty of Science and Natural Resources, Universiti Malaysia Sabah, Jalan UMS, 88400 Kota Kinabalu, Sabah MALAYSIA.

[3]Department of Physics, College of Science, University of Anbar, Anbar, IRAQ

Corresponding author: saturi@ums.edu.my (S.Baco)

Abstract

Mechanical properties of soft magnetostrictive FeCo-based thin films is one of the critical properties along with their magnetic properties. To fully exploit their potential in magnetic-microelectromechanical (MagMEMs) application, the elastic and inelastic properties as well as the strength need to be considered. This paper presents the mechanical properties of soft magnetostrictive FeCoCr films at varied Cr concentrations from 2.6 to 9.6 at.% fabricated by RF Sputtering. Nanoindentation was performed to determine the hardness, elastic recovery, Young's modulus, and the yield strength of the FeCo and FeCoCr films. Although the Cr substitutions slightly reduced the hardness and the Young's Modulus, the yield strength of the films improved, with a maximum of 1014 MPa for 9.6 at.% Cr. This suggests that the Cr atoms were responsible for inhibiting the dislocations motion in the soft magnetostrictive FeCo-based films and helped to overcome the brittleness of the FeCo.

Keywords: mechanical properties, nanoindentation, thin film.

1. Introduction

Soft magnetostrictive materials with low coercivity (H_c < 200 A/m), high hardness and yield strength are well-suited for use in magnetic-microelectromechanical (MagMEMs) sensors, which can operate at both room and elevated temperatures [1],[2],[3]. As the behaviours of bulk alloys can differ from thin films due to the nanoscale film thickness, investigating the mechanical properties are crucially important to understand their fundamental features. However, developing such material is challenging because one needs to improve the mechanical properties without sacrificing the softness of the magnetic materials. It was previously shown that the magnetic properties of FeCo were degraded (*i.e.* saturation magnetization reduced while the coercivity increased) when the ductility of this material was improved when alloyed with 2 wt% vanadium [4]. Previous studies also found that as-deposited FeCo films had large magnetostriction constants (λ_s > 60 ppm) and coercivity (H_c > 10 kA/m) [5],[6],[7]. The FeCo in the ordered structure, nevertheless is brittle at room temperature [8].

Numerous studies have been undertaken in investigating the mechanical properties of a wide range of materials from bulk to amorphous thin films [9],[10]. The mechanical properties of bulk materials are generally measured using the standard tensile and bend test [11], while for thin films in the nanoscale range, the hardness, elastic modulus, and elastic recovery are

typically extracted using nanoindentation where loads are measured as a function of penetration depth [12], [13]. However, characterization of mechanical behaviour, particularly for soft magnetostrictive films of FeCo doped with Cr in the nanoscale range, have not been studied. Poor mechanical strength of soft magnetostrictive materials may limits their application in MagMEMs sensors, which are exposed to mechanical stresses. Therefore, this paper aims to develop a fundamental understanding of the mechanical properties of soft magnetostrictive FeCoCr films to exploit their potential. Results are presented on how the magnetic properties, film hardness, Young's modulus, elastic recovery, and yield strength of FeCo films vary when they are doped with Cr.

2. Experimental methods

FeCo and FeCoCr thin films were grown onto silicon substrate via RF sputtering at an optimised pressure of 4.8 mTorr and sputtering power, 75 W. Cr foils target with purity 99.99%, were placed on the top of the FeCo (47:53) target. To vary the Cr compositions, a maximum of four Cr pieces were used with each size of 2.5 mm x 2.5 mm x 1 mm. The Cr concentrations (2.6 at. %, 5.6 at.%, 7.2 at.%, and 9.6 at.%) were confirmed using a SEM Model BMS Tescan Vega3 LMU equipped with EDX Oxford Instrument at an applied voltage of 10 kV. Glancing angle X-Ray Diffraction (GA-XRD PANanalytical X-Pert Powder) with Cu-Kα ($\lambda = 1.540598$ Å) measurements were used to determine the structure of the FeCo and FeCoCr films, including the lattice constants from the (110) peak. Films' thicknesses were measured using an Atomic Force Microscopy (AFM DimensionTM 3000). The thicknesses were found to be 604 nm (2.6 at.% Cr), 590 nm (5.6 at.%), 600 nm (7.2 at.%) and 601 nm (9.6 at.%). The mechanical properties; hardness, H and reduced modulus of elasticity, E_r of the films were determined by performing the nanoindentation technique using a TI 950 Triboindenter Hysitron. For such measurements, it is essentially that the film thicknesses are larger than the radius of the nanoindentation tip (120 nm). Thus, before measuring the mechanical properties of the films, nanoindentation on the silicon substrate was conducted to ensure that the films' hardness was not influenced by the Si substrate. Hence, this study also characterized the mechanical properties of a bare 360 µm Si substrate. A Berkovich tip supplied by Bruker was used with radius 120 nm, angle, $\varphi = 142.3^0$, Young's modulus, $E_Y = 1140$ GPa and Poisson's ratio, $\upsilon = 0.07$. The tip was calibrated on fused quartz, with a known elastic modulus. A series of nanoindentation were performed with a partial unload, the measurement consisted of three segments: 5 s for loading, 5 s hold at the load maximum and 5 s for unloading. The maximum load applied was 13000 µN. AFM images of the indentations area were taken after the nanoindentations were performed. The films' yield strength, σ_y was determined by performing indentation using the Nanotest Vantage equipment, with an applied load of 100 mN. To measure this property, a spherical tip with radius 19 µm was used. One advantage of using the spherical tip to measure the yield strength is that one can determine the material response from initial elasticity to initial plasticity regions, then until post-yield at finite plastic strain [14]. A series of indentation involving 30 cycles were made onto several areas of interest on each sample. The load and displacement data curve were subsequently analysed based on the Field and Swain measurement [15] allowing extraction of the yield strength from the flow stress-flow strain plot.

3. Results and discussion

3.1 Structure and surface morphology properties

Fig. 1. demonstrates the difference in the XRD peaks of the FeCo and FeCoCr with the highest Cr composition (at.9.6%) films with a comparable thickness; 603 nm and 601 nm, respectively. While the FeCo film displays a sharper peak with higher intensity at $2\theta{\sim}44.7^0$, the FeCoCr film in contrast exhibits a lower intensity peak at $2\theta{\sim}44.3^0$. The FeCo peak at ${\sim}44.7^0$ corresponds to a strong BCC (110) texture within the film, which is consistent with the literature [16]. The lattice constants, a, for these two films were determine from the (110) peak. It was found that the FeCo film lattice constant was $a = 2.863 \pm 0.002$ Å, so larger than the bulk FeCo lattice constant (2.855 Å) [17], suggesting in-plane compressive stress. Meanwhile, the lattice constant of the FeCoCr film, $a = 2.888 \pm 0.001$ Å indicates that the Cr dopants into the FeCo film further increased the lattice constant, plus the additional Cr contributed to inhomogenous stresses within the films, which gave rise to the broader peak observed.
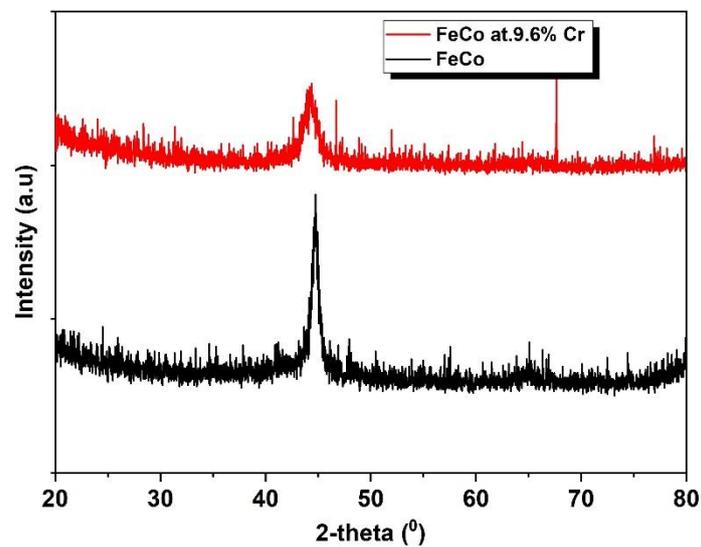

Fig. 1: Comparison on X-Ray diffraction profiles between the FeCo and FeCoCr films at the highest Cr concentration.

To further study the morphology differences between the FeCo and FeCoCr films, the surface morphology analysis was examined by using AFM. As illustrated in Fig.2a, the surface roughness of the FeCo film is larger ($R_a = 1.657 \pm 0.004$nm) with the grains more noticeable than the roughness of the FeCoCr films ($R_a = 0.48 \pm 0.01$ nm) with no grains being identified (Fig.2b). Thus, the FeCoCr films are smoother than the FeCo film.

$R_a = 1.657 \pm 0.004$ nm (a)

$R_a = 0.48 \pm 0.01$ nm (b)
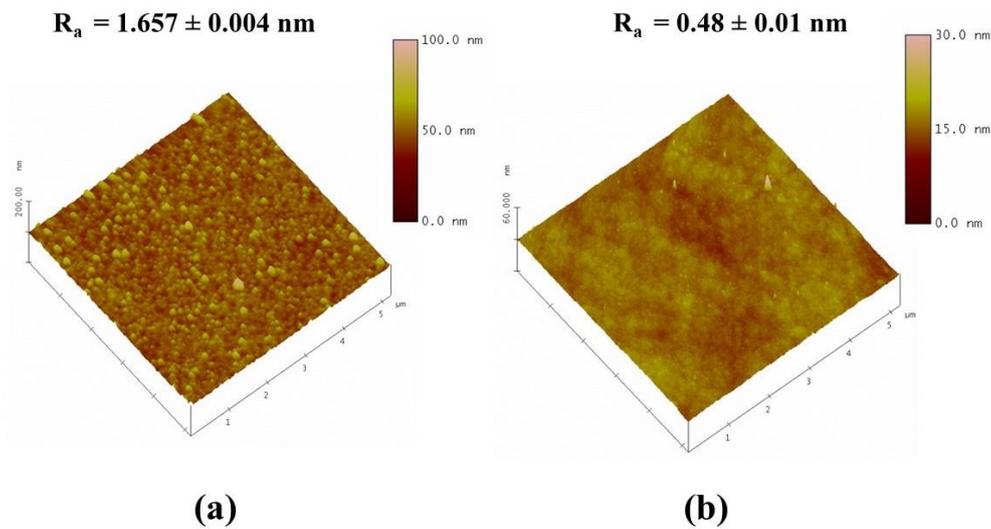
Fig.2: The comparison on the AFM images of the surfaces morphologies of the (a) FeCo and (b) FeCoCr films. Scan size of 5 µm x 5 µm.

3.2 Nanoindentation analysis

When taking nanoindentation measurements, the tip indenter makes contact into an elastic material, such that surface deformation may occur, either as sink-in or pile-up around the indenter. This can lead to an overestimation of the hardness and modulus properties up to 60% and 16%, respectively, depending on the amount of pile-up [18]. For this reason, it is essential to study the pile-up or sink-in behaviour of the FeCo and FeCoCr films and determine if they have undergone either of these effects. AFM images were taken after the indentations were performed. Fig.3 displays a cross-sectional analysis and the 3D images of four indentations made on the FeCo film. From the 3D images, no sink-in event was observed. Nonetheless, a small pile-up occurred on one side of the indenter. The measured height of the pile-up on FeCo film was found to be about 13.21 nm. While for the FeCoCr (9.6 at.% Cr) film, a significant pile-up event occurred as indicated in Fig.4 with measured heights varying from 15.27 nm to 24.41 nm. The amount of pile-up depends on how far the dislocations move into the material [19].
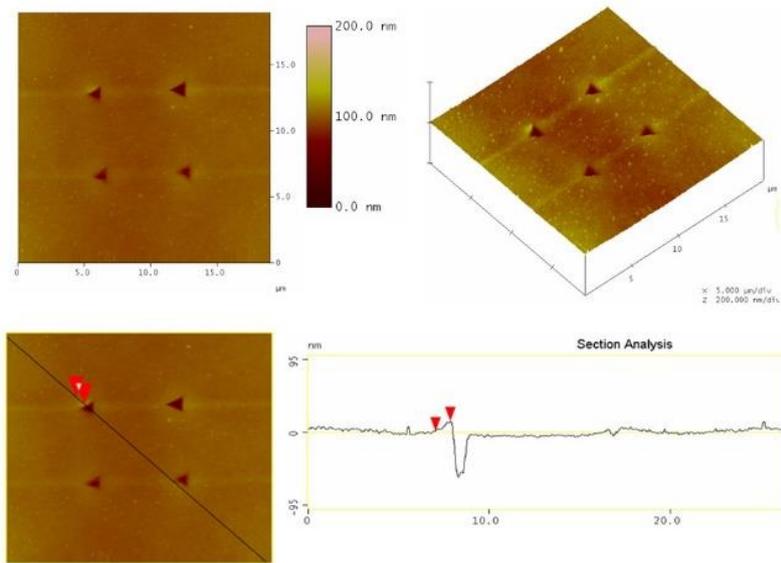
Fig.3: AFM images of the 3D view (on the top-right) and a cross-section analysis (on the bottom) showing a small pile-up has occurred on one-side indenter on the FeCo films. Data scale is 200 nm with the scan size of 19 µm x 19 µm.
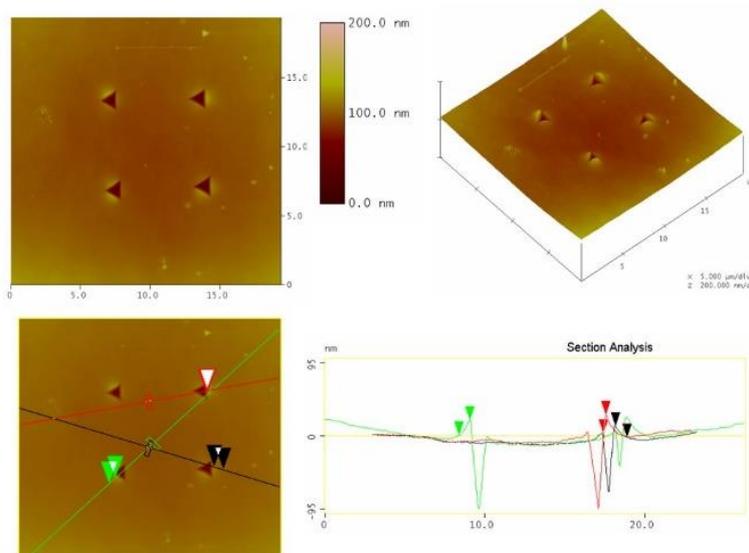
Fig.4: AFM images of the 3D view (on the top-right) and a cross-section analysis (on the bottom) showing significant pile-up occurred on the four-sides indenter on the FeCoCr films (9.6 at.% Cr). Data scale is 200 nm with the scan size of 19 µm x 19 µm.

For the nanoindentation measurement, the unloading curve of force-displacement (P-h) (Fig. 5) were fitted using a method developed by Oliver and Pharr [12],[13] leading to the extraction

of the hardness, H and reduces modulus of elasticity, E_r. These two properties, are derived from the following equations:

$$H = \frac{P_{max}}{A} \qquad\qquad (eq.1)$$

$$E_r = \frac{\sqrt{\pi}}{2} \beta \frac{S}{A} \qquad\qquad (eq.2)$$

where H = hardness; A = contact area; P_{max} = load at maximum, E_r = reduced modulus of elasticity; β = correction factor; S = elastic unloading stiffness.

Determination of E_r then allow an estimate of the Young's modulus, E_f of sample under test, which is given by:

$$\frac{1}{E_r} = \frac{1-\upsilon_f}{E_f} + \frac{1-\upsilon_i}{E_i} \qquad\qquad (eq.3)$$

where υ_i = Poisson ratio of indenter (0.07), υ_f= Poisson ratio of film; E_i = Young's modulus of indenter (1140 GPa); E_f = Young's modulus of film, respectively.
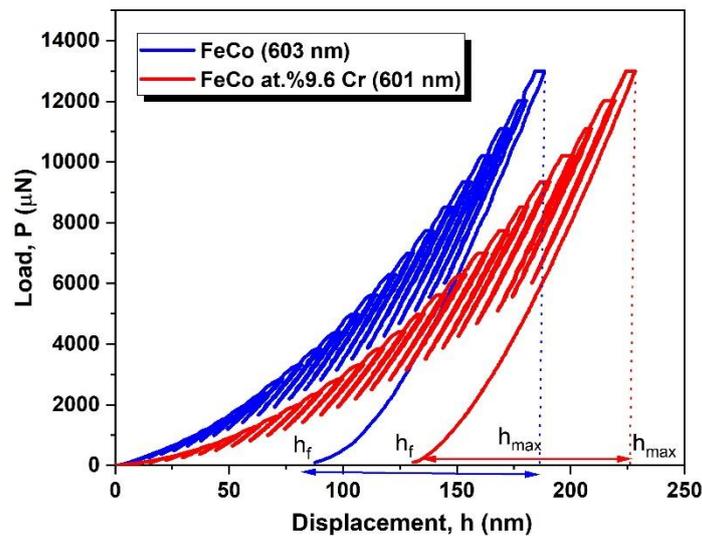

Fig 5: A comparison of load-displacement curves between the FeCo (603 nm) and the representative film of FeCoCr (9.6 at.% Cr). Also shown in the curves are the maximum displacement, h_{max} and the final depth, h_f of the indenter during unloading.

The hardness, H, as a function of penetration depth, h_c for the Si substrate, FeCo and FeCoCr films for different Cr concentration are presented in Fig.6. There is a pronounced increase in the hardness of Si at the lower penetration depths between 7 nm and 20 nm. An increase in the hardness at smaller depth is usually associated with the radius of the indenter tip. The hardness

value becomes irregular when the contact depth approaches nearly a-third of the radius tip [20]. It is also possible that tip rounding is contributing to a sudden increase in the hardness at the lower depth. For Si, a constant hardness value was observed for the contact depth ranging from 20 nm to 40 nm. After this range, the hardness increases gradually with increasing depth. Nevertheless, the increment in the hardness is still within the error bars, therefore the Si hardness was calculated from the displacement between 20 nm to 140 nm and determined to be 16 ± 1 GPa, which was higher than the hardness (12.75 GPa) reported in the literature [21]. It is important to note that the average hardness and reduced modulus of elasticity for all films were calculated within the range where the plateau occurred. The error bars in the plots represent the standard errors calculated from the series of nanoindentations.

Fig. 6. also shows that there was no contribution from the substrate as the indenter depth increased, the hardness for all the films remained constant. The FeCo films show higher hardness 15.1 ± 0.4 GPa compared to the FeCoCr films. The average hardness value of the FeCo films were taken between 20 nm and 110 nm contact depth. For the FeCo films doped with Cr, the hardness was found in the range between 12 GPa and 13.5 GPa, with the 7.2 at.% Cr film having the lowest hardness, $H = 12.2 ± 0.1$ GPa and the 5.6 at.%Cr film having the highest hardness, $H = 13.5 ± 0.2$ GPa. Meanwhile, the films with 2.6 at.% Cr and 9.6 at% Cr have almost the same hardness, which are 13.3± 0.2 GPa and 13.2 ± 0.2 GPa, respectively. Thus, the hardness of FeCoCr is independent of the Cr concentration. One plausible reason for a significant difference in the hardness between FeCo and FeCoCr is due to soft material properties of the FeCoCr films that lead to the material effect (pile-up) revealed in AFM analysis (Fig. 4).

Fig.7 shows the plot of reduced modulus of elasticity, E_r of the films and Si substrate as a function of indenter displacement. The average E_r of Si was lower (165 ± 2 GPa) than the FeCo films ($E_r = 181 ± 2$ GPa). There was a significant difference in this parameter between the FeCoCr films with the highest and lowest Cr concentration, such that E_r was found to be 170 ± 1 GPa for the 9.6 at.% Cr film and $E_r = 150 ± 1$ GPa, for the 2.6 at.% Cr film. The E_r was found to be constant at 169 ± 1 GPa for both films with 5.6 at.% Cr and 7.2 at.% Cr. Overall, adding Cr into FeCo lowered the E_r, as the E_r values of the FeCoCr films were all smaller than the E_r obtained for the FeCo film.
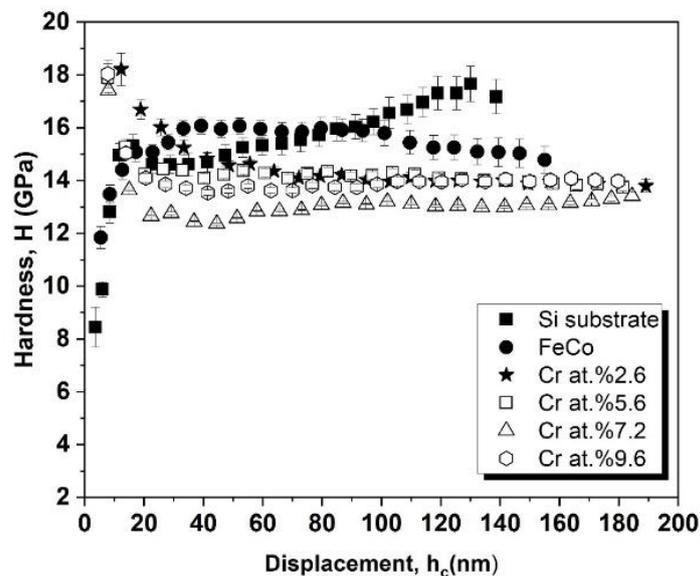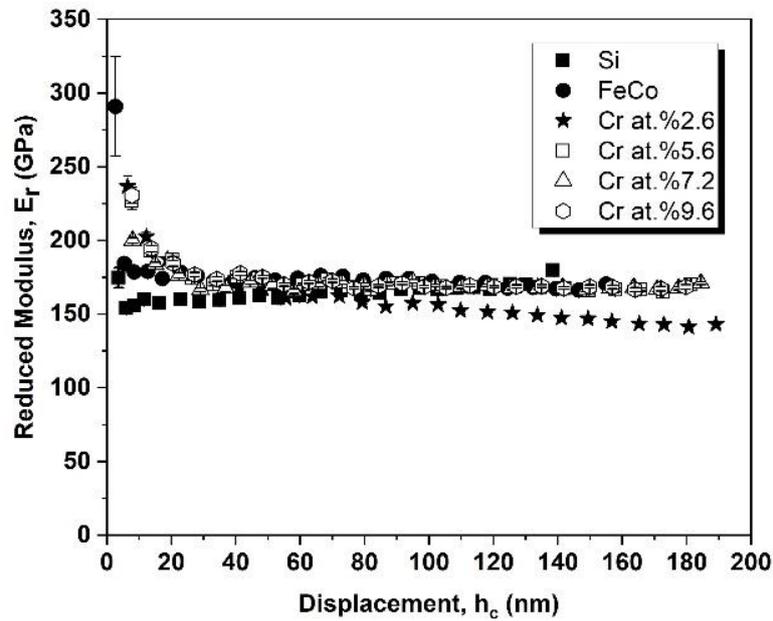
Fig.7: Reduced modulus, E_r as a function of indenter displacement of Si substrate, FeCo and FeCoCr films for different Cr concentrations.

Using Equation 3, the Young's modulus of the films, E_f were determined. Table 1 summarized the Young's modulus of the FeCoCr with range of Cr concentrations along with the hardness and the reduced modulus of the elasticity of bare silicon substrate and the FeCo. It shows that the 2.6 at. % Cr film had the lowest average of Young's modulus, E_f = 144 ± 1 GPa. For the films with Cr concentrations between 5.6 at.% Cr and 9.6 at.% Cr, the average E_f were the same within error. The Young's modulus obtained for the FeCo film was higher (E_f = 167 ± 1GPa) compared to the FeCoCr films. This could be ascribed to the different microstructure as determined from the XRD and the surface roughness from the AFM images, hence the addition of Cr into FeCo has changed the elastic properties of the films. Another mechanical parameter which can measured directly from the load-displacement plot is the elastic recovery, h_e, which can be calculated from the difference between the maximum displacement, h_{max}, and the final depth, h_f. The elastic recovery, h_e for the FeCoCr film was found to be slightly higher h_e = 95.2 ± 0.3 nm than the FeCo film (h_e = 92.7 ± 0.2 nm), reflecting the softer nature of the FeCoCr films, as they are easier to deform compared to the harder FeCo films.

Table 1: The Young's modulus and other mechanical parameters of silicon substrate, FeCo and FeCoCr at variation of Cr concentrations determined from nanoindentation technique.

Sample	Young's modulus, E_f (GPa)	Reduced modulus of elasticity, E_r (GPa)	Hardness, H (GPa)
Si substrate	155 ± 2	165 ± 2	16 ± 1
FeCo	167 ± 1	181 ± 2	14.8± 0.2
FeCo (Cr at.2.6%)	144 ± 1	150 ± 1	13.3 ± 0.2
FeCo (Cr at.5.6%)	157 ± 1	169 ± 1	13.5 ± 0.2
FeCo (Cr at.7.2%)	156 ± 1	169 ± 1	12.2 ± 0.1
FeCo (Cr at.9.6%)	157 ± 1	170 ± 1	13.2 ± 0.2

To extend an understanding on the mechanical behaviour of the FeCoCr films, the yield strength, σ_y has been studied. As the stress-strain curve measured in this study do not show a perfect curve like those for the standard tensile measurement of bulk material, thus a method of a linear fit between the elastic and plastic region was used to estimate this parameter. Fig.8 compares the yield strength, σ_y between the FeCo and FeCoCr samples. The error bars in the plot represents the standard error calculated from a series of indentation for each sample. It is shown that the FeCo film had a $\sigma_y = 828 \pm 75$ MPa. For the addition of Cr into FeCo, it is clearly seen that the yield strength, σ_y decreases initially from 821 ± 58 MPa (sample at.%2.6 Cr) to 770 ± 46 MPa as the concentrations increases to at.% 5.6 Cr. Then, the σ_y is considerably enhanced to the value of 1014 ± 45 MPa for at.%9.6 Cr film. A maximum σ_y was observed at a concentration of at.%9.6 Cr indicated that there was an optimum Cr content can lead to the enhancement of σ_y. By comparing this value, which was higher than the σ_y of FeCo implies that the incorporation of Cr atoms at.% 9.6 into FeCo can strengthen the films, by inhibiting the movement of dislocations. The FeCoCr films have an amorphous/nanocrystalline microstructure, such that the atomic disorder causes discontinuity of any further dislocation motions [22], [23]. It also been reported that addition of Cr into ferromagnetic shape memory alloy of Ni-Mn-In thin films have shown a considerably improve the strength of the $Ni_{50.4}$ $Mn_{34.96}$ $In_{13.56}$ $Cr_{1.08}$ which attributed by a large number of grain boundaries acts as a barrier of the dislocations [24].
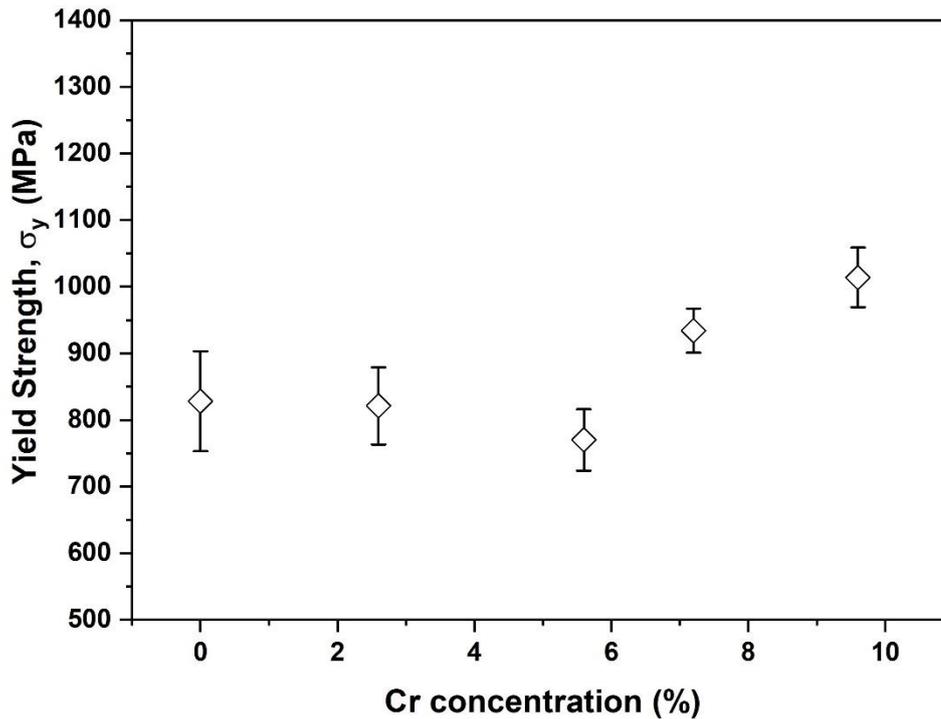
Fig.8: The measured yield strength, σ_y of the FeCo and FeCoCr films as function of Cr concentrations.

4. Conclusion

In summary, we have provided a fundamental investigation into the mechanical properties of FeCo films doped with different Cr concentrations by nanoindentation. The hardness and the Young's modulus of the FeCo films reduced slightly with Cr substitutions due to the different microstructure and pile-up events, which occurred in these films. However, the yield strength was enhanced to a maximum value 1014 MPa by doping with 9.6 at.% Cr, which potentially helps to overcome the brittleness of the FeCo. Results obtained from this study, help to facilitate the operation limits and reliability of FeCo and FeCoCr films in MEMS devices.

References

[1]   K. S. Chan, H. Ji, X. Wang, S. J. Hudak, and B. R. Lanning, "Mechanical properties and interface toughness of FeCo thin films on Ti-6Al-4V," *Mater. Sci. Eng. A*, vol. 422, no. 1–2, pp. 298–308, 2006, doi: 10.1016/j.msea.2006.02.035.

[2]   E. W. H. and P. J. W. M R J Gibbs, "Magnetic materials for MEMS applications," *J. Phys. D. Appl. Phys.*, vol. 37, pp. R237–R244, 2004, doi: https://doi.org/10.1088/0022-3727/37/22/R01.

[3]   H. S. Lee and C. Cho, "Study on advanced multilayered magnetostrictive thin film coating techniques for MEMS application," *J. Mater. Process. Technol.*, vol. 201, no. 1–3, pp. 678–682, 2008, doi: 10.1016/j.jmatprotec.2007.11.255.

[4]   R. S. Sundar, S. C. Deevi, and B. V. Reddy, "High strength FeCo-V intermetallic alloy: Electrical and magnetic properties," *J. Mater. Res.*, vol. 20, no. 6, pp. 1515–1522, 2005, doi: 10.1557/JMR.2005.0206.

[5]   M. D. Cooke, M. R. J. Gibbs, and R. F. Pettifer, "Sputter deposition of compositional gradient magnetostrictive FeCo based thin films," *J. Magn. Magn. Mater.*, vol. 237, no. 2, pp. 175–180, 2001, doi: 10.1016/S0304-8853(01)00510-8.

[6]   N. A. Morley, S. Rigby, and M. R. J. Gibbs, "Anisotropy and magnetostriction constants of nanostructured FeCo films," *J. Optoelectron. Adv. Mater. Symposia*, vol. 1, pp. 109–113, 2009.

[7]   S.Kotapati, A. Javed, N.Reeves-McLaren, M.R.J.Gibbs, and N.A.Morley, "Effect of the Ni81Fe19 thickness on the magnetic properties of Ni81Fe19/Fe50Co50 bilayers," *J. Magn. Magn. Mater.*, vol. 331, pp. 67–71, 2013, doi: https://doi.org/10.1016/j.jmmm.2012.11.022.

[8]   E. P. George, A. N. Gubbi, I. Baker, and L. Robertson, "Mechanical properties of soft magnetic FeCo alloys," *Mater. Sci. Eng. A*, vol. 329–331, pp. 325–333, 2002, doi: 10.1016/S0921-5093(01)01594-5.

[9]   A. K. Battu and C. V. Ramana, "Mechanical Properties of Nanocrystalline and Amorphous Gallium Oxide Thin Films," *Adv. Eng. Mater.*, vol. 20, no. 11, pp. 1–10, 2018, doi: 10.1002/adem.201701033.

[10]   M. Noroozi, A. Petruhins, G. Greczynski, J. Rosen, and P. Eklund, "Structural and mechanical properties of amorphous AlMgB14 thin films deposited by DC magnetron sputtering on Si, Al2O3 and MgO substrates," *Appl. Phys. A Mater. Sci. Process.*, vol. 126, no. 2, pp. 1–6, 2020, doi: 10.1007/s00339-020-3316-z.

[11]   Y. Sasaki, M. Ciappa, T. Masunaga, and W. Fichtner, "Accurate extraction of the mechanical properties of thin films by nanoindentation for the design of reliable MEMS," *Microelectron. Reliab.*, vol. 50, no. 9–11, pp. 1621–1625, 2010, doi: 10.1016/j.microrel.2010.07.119.

[12]   G. M. Pharr and W. C. Oliver, "Measurement of Thin Film Mechanical Properties Using Nanoindentation," *MRS Bull.*, vol. 17, no. 7, pp. 28–33, 1992, doi: 10.1557/S0883769400041634.

[13]   W. C. Oliver and G. M. Pharr, "Measurement of hardness and elastic modulus by instrumented indentation: Advances in understanding and refinements to

methodology," *J. Mater. Res.*, vol. 19, no. 1, pp. 3–20, 2004, doi: 10.1557/jmr.2004.19.1.3.

[14]   S. Pathak and S. R. Kalidindi, "Spherical nanoindentation stress-strain curves," *Mater. Sci. Eng. R Reports*, vol. 91, pp. 1–36, 2015, doi: 10.1016/j.mser.2015.02.001.

[15]   J. S. Field and M. V. Swain, "Determining the mechanical properties of small volumes of material from submicrometer spherical indentations," *J. Mater. Res.*, vol. 10, no. 1, pp. 101–112, 1995, doi: 10.1557/JMR.1995.0101.

[16]   T. Nakajima *et al.*, "Effect of Annealing on Magnetostrictive Properties of Fe - Co Alloy Thin Films," *Mater. Trans.*, vol. 55, no. 3, pp. 556–560, 2014.

[17]   R. . Bozorth, *Ferromagnetism*. D. Van Nostrand Co. Inc, 1951.

[18]   A. Bolshakov and G. M. Pharr, "Influences of pileup on the measurement of mechanical properties by load and depth sensing indentation techniques," *J. Mater. Res.*, vol. 13, no. 4, pp. 1049–1058, 1998, doi: 10.1557/JMR.1998.0146.

[19]   N. Moharrami and S. J. Bull, "A comparison of nanoindentation pile-up in bulk materials and thin films," *Thin Solid Films*, vol. 572, pp. 189–199, 2014, doi: 10.1016/j.tsf.2014.06.060.

[20]   A. C. Fischer-Cripps, *Nanoindentation [electronic Resource]. 3rd ed. Mechanical Engineering Series*, 3rd ed. New York ; London : Springer, 2011.

[21]   R. Saha and W. D. Nix, "Solt films on hard substrates - Nanoindentation of tungsten films on sapphire substrates," *Mater. Sci. Eng. A*, vol. 319–321, pp. 898–901, 2001, doi: 10.1016/S0921-5093(01)01076-0.

[22]   M. Nagumo and M. Umemoto., "The Hall-Petch relationhip in nanocrystalline materials," *Mater. Trans. JIM*, vol. 38, no. 12, pp. 1033-1039., 1997.

[23]   S. N. Naik and S. M. Walley, "The Hall–Petch and inverse Hall–Petch relations and the hardness of nanocrystalline metals," *J. Mater. Sci.*, vol. 55, no. 7, pp. 2661–2681, 2020, doi: 10.1007/s10853-019-04160-w.

[24]   H. S. Akkera and D. Kaur, "Effect of Cr addition on the structural, magnetic and mechanical properties of magnetron sputtered Ni–Mn–In ferromagnetic shape memory alloy thin films," *Appl. Phys. A Mater. Sci. Process.*, vol. 122, no. 12, pp. 1–9, 2016, doi: 10.1007/s00339-016-0528-3.